Land subsidence rebound detected via multi-temporal InSAR and ground truth data in Kalochori and Sindos regions, Northern…

Article *in* Engineering Geology · May 2016

DOI: 10.1016/j.enggeo.2016.05.017

CITATIONS
0

READS
63

6 authors, including:

Nikos Svigkas
Aristotle University of Thessaloniki
6 PUBLICATIONS **5** CITATIONS
SEE PROFILE

Paraskevas Tsangaratos
National Technical University of Athens
45 PUBLICATIONS **143** CITATIONS
SEE PROFILE

Anastasia A. Kiratzi
Aristotle University of Thessaloniki
136 PUBLICATIONS **2,756** CITATIONS
SEE PROFILE

Kontoes Charalabos
National Observatory of Athens
141 PUBLICATIONS **688** CITATIONS
SEE PROFILE

Engineering Geology 209 (2016) 175–186

Contents lists available at ScienceDirect

Engineering Geology

journal homepage: www.elsevier.com/locate/enggeo

Land subsidence rebound detected via multi-temporal InSAR and ground truth data in Kalochori and Sindos regions, Northern Greece

Svigkas Nikos [a,b,*], Papoutsis Ioannis [b], Loupasakis Constantinos [c], Tsangaratos Paraskevas [c], Kiratzi Anastasia [a], Kontoes Charalambos (Haris) [b]

[a] Department of Geophysics, Aristotle University of Thessaloniki, 54124 Thessaloniki, Greece
[b] Institute of Space Applications and Remote Sensing, National Observatory of Athens, Metaxa & Vas. Pavlou, 15236 Athens, Greece
[c] Laboratory of Engineering Geology and Hydrogeology, Department of Geological Sciences, School of Mining and Metallurgical Engineering, National Technical University of Athens, Zographou Campus, Heroon Polytechniou 9, 15780 Athens, Greece

ARTICLE INFO

Article history:
Received 10 November 2015
Received in revised form 21 March 2016
Accepted 28 May 2016
Available online 30 May 2016

Keywords:
Detected surface rebound
Remote Sensing
Ground truth data

ABSTRACT

Land subsidence in the broader Kalochori village region, at the west side of Thessaloniki, has been recorded since the early 1960s reaching gradually, next to the coastline, maximum values of 3–4 m. Temporal monitoring of terrain movements are exploited and combined with in-situ data to enhance understanding of the deformation signals. Persistent Scatterer Interferometry (PSI) and Small Baseline Subset (SBAS) multi-temporal Interferometric approach are applied for the analysis of a 20 year ERS 1, 2 and ENVISAT dataset. The velocities estimated for the ERS dataset are in excellent accordance with previous studies, depicting subsidence with magnitude up to 35 mm/year. The intriguing output of the ENVISAT data archive (2003–2010) shows that, during the second decade, there was a change in motion trend, from subsidence to uplift. The fact that this uplifting trend of the second decade is well correlated with hydrogeological data of the area that show a synchronous rise of the aquifer level, verifies the dominating driver of the human factor concerning the land subsidence phenomena taking place the last 55 years. This conclusion is further supported by the fact that since 2007 the uplifting signal becomes smoother, following the smoother recovery of the aquifers.

1. Introduction

The use of SAR Interferometry techniques can reveal and map the surface deforming areas with great precision (e.g. Fruneau and Sarti, 2000; Le Mouelic et al., 2002; Massonnet et al., 1993; Wright and Stow, 1999). Groundwater level variation can have an impact at the surface deformation (e.g. Galloway et al., 1998; Ikehara and Phillips, 1994) and Interferometric Synthetic Aperture Radar (InSAR) techniques have been among the tools successfully applied for the study of deformation due to the activity of aquifer systems (e.g. Amelung et al., 1999; Bell et al., 2008; Galloway and Hoffmann, 2007; Galloway et al., 1998; Zhong and Danskin, 2001). Worldwide, numerous studies have highlighted the occurrence of subsidence due to groundwater overpumping (e.g. Phien-wej et al., 2006; Raspini et al., 2013, Taniguchi et al., 2009). On the contrary, uplifting deformation due to natural rebound has been reported only for limited sites, as for example in the work of Chen et al. (2007) in Metropolitan Taipei Basin or Ishitsuka et al. (2014) at the Bangkok plain, who reported the phenomenon at a previously subsided site.

The urban expansion and the economic activities related with everyday life, affect the natural evolution of the landscape and the physical processes. In Greece, this interaction is most pronounced in Kalochori and Sindos, two sites that are strongly related to industrial activities, especially related to the metropolitan city of Thessaloniki (Fig. 1). At these sites, a subsiding trend was first detected in the 1960s and was highlighted from studies using ground truth techniques (Andronopoulos et al., 1990; Doukas et al., 2004; Hatzinakos et al., 1990; Loupasakis and Rozos, 2009; Rozos and Hatzinakos, 1993; Stiros, 2001) but it was after 2000 and the advent of satellite technology that boosted more detailed studies (Costantini et al., 2016; Mouratidis et al., 2009; Psimoulis et al., 2007; Raspini et al., 2014; Raucoules et al., 2008). ERS 1, 2 data from the 90s successfully verified the subsidence phenomena adding new information on their distribution and deformation rate.

A change in the sense of motion, was first identified in a preliminary ENVISAT SAR data analysis, for the post 2000 period, which indicated that both Sindos and Kalochori are uplifting (Svigkas et al., 2015). The further investigation of this phenomenon and its mechanism is the subject of this work. To this end, the approach applied seeks to exploit the advantages of repeat pass space born SAR Interferometry and apply the well-established techniques of Persistent Scatterer Interferometry (PS) and Small Baseline Subset (SBAS) for the detection of surface

* Corresponding author at: Department of Geophysics, Aristotle University of Thessaloniki, 54124, Thessaloniki, Greece.
E-mail address: svigkas@geo.auth.gr (S. Nikos).

http://dx.doi.org/10.1016/j.enggeo.2016.05.017
0013-7952/

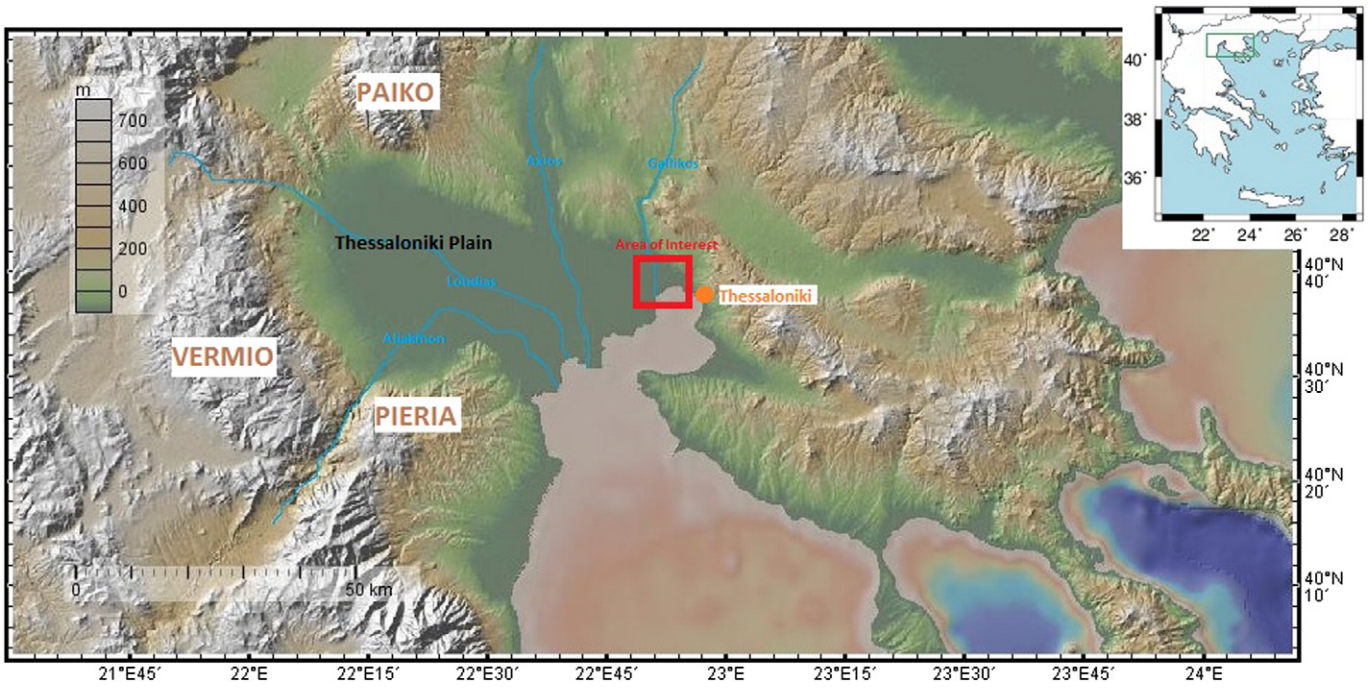

Fig. 1. Location map of the broader area of interest. Red rectangle shows the study area of Kalochori and Sindos. The inset map of Greece, presents the location of the study area with a green rectangle. For the elevation data the shuttle radar topography mission (SRTM) DEM was used. (For interpretation of the references to colour in this figure legend, the reader is referred to the web version of this article.)

deformation. The velocities presented here, constitute a combined result of these two techniques and they are cross-checked with hydrogeological data. Combining SAR Interferometry with hydrogeology leads to a validation of the remote sensing results and to an interpretation of the driver mechanism.

2. The subsidence history of Kalochori and Sindos

Kalochori and Sindos are located at Thessaloniki plain, which extends at the western part of Thessaloniki city. The Thessaloniki plain, the largest deltaic plain in Greece (~2000 km^2), is surrounded by mount Vermio (2100 m) and Pieria hill from the south and mount Paiko (1600 m) from the north (Fig. 1). The plain is crossed by the rivers Axios, Loudias and Aliakmon, which constitute an important geomorphological factor that formed the site as it is today.

The area of Kalochori and Sindos used to be a delta some thousands years ago (Psimoulis et al., 2007). Numerous archaeological discoveries, like the remains of the ancient port of Pella (Petsas, 1978), which was a harbour at the times of Alexander the Great, give insights about the continuously changing geomorphology. During the years, the human factor

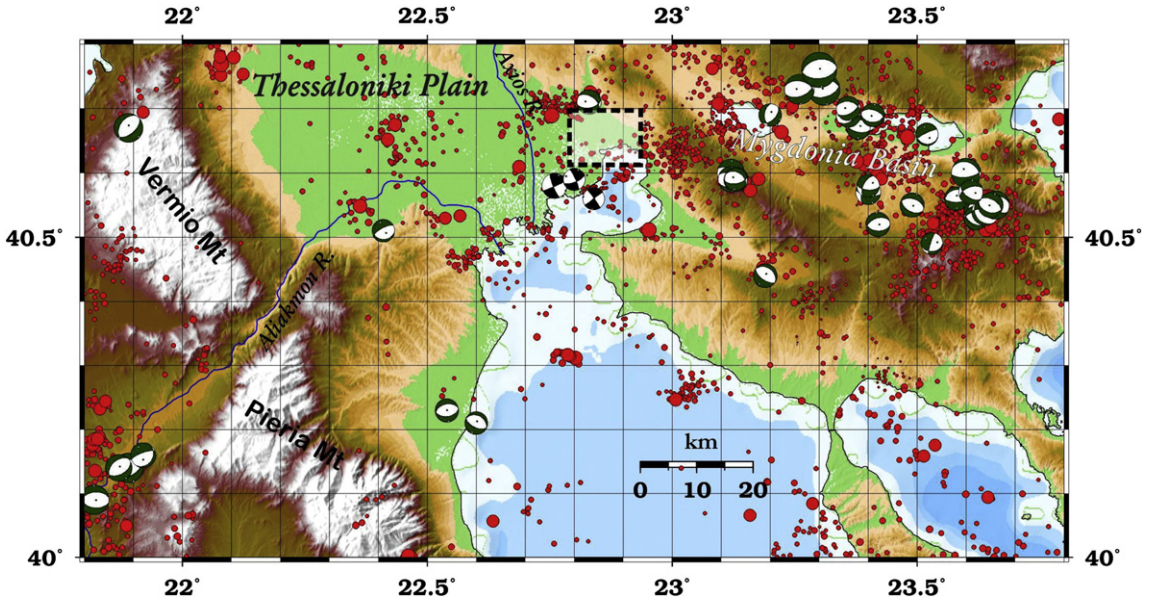

Fig. 2. Seismicity (red circles) for the broader area. The seismicity data cover the period 1980–2016 and the size of the symbols scales with magnitude. Most of the modern seismicity is connected with the Mygdonian Basin. The beach balls denote the focal mechanisms of the stronger (Mw > 4) earthquakes of the region, and as seen the presently acting stress field denoted ~N-S extension. The dashed rectangle marks the region under study. (For interpretation of the references to colour in this figure legend, the reader is referred to the web version of this article.)

Fig. 3. Failures at Kalochori region resulted from the subsidence phenomena. a) Pipe upheaval, b) Damages at the Electricity Network. The photographs were taken in July 2012.

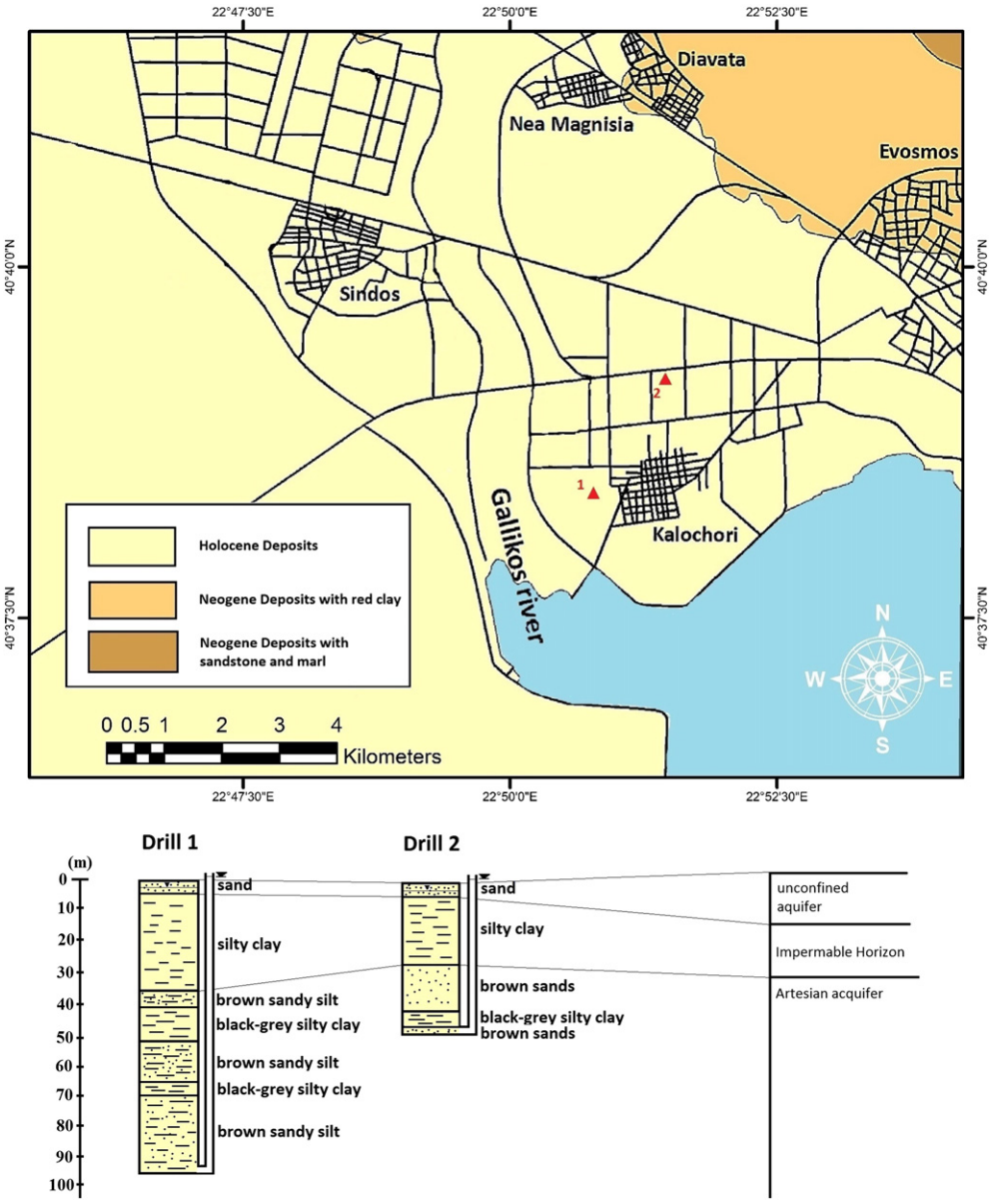

Fig. 4. Geological map of the area (modified after IGME, 1978 and Raspini et al., 2014). With red triangles two drills are denoted. Bellow the map the Drills` logs and the aquifers succession are presented. Drill loggings are from Andronopoulos et al. (1990). (For interpretation of the references to colour in this figure legend, the reader is referred to the web version of this article.)

had the key-role for the evolution of morphology at this particular plain (Sivignon, 1987). Indicative examples of human intervention at the plain, since the ancient times, would include: diversion and alignment of rivers, the development of an irrigation network, construction of dams, overpumping of the underwater aquifers (Kapsimalis et al., 2005). The formation of the basin bearing the present morphological features was the result of the intense active tectonics of the Upper Pleistocene (Syrides, 1990).

The modern seismicity and tectonic activity in the broader region is summarized in Fig. 2. The focal mechanisms (beach-balls) of the stronger earthquakes (Mw > 4), depicted in the figure, clearly show these are mainly located in the Mygdonian basin, and are all connected with normal faulting. The present day stress field in the broader region suggests approximately N-S extension, in accordance with the E-W strike of major active structures (Kiratzi, 2014 and references therein). The region under study (dashed rectangle) is related with sparse microseismicity and the available focal mechanisms for a moderate sequence which occurred in 2012 close to region indicate strike-slip motions along NE-SW trending planes.

At coastal areas in general, the phenomenon of subsidence can remarkably raise the risk of flooding. Delta municipality (where Kalochori and Sindos belong to) is just a few meters above the sea level and the coastal front of Kalochori lies below it. In 1964 there was the first detection of subsidence in the form of seawater invasion. At 1965 an intensive rainfall took place, causing seawater inundation threatening the houses located at the southern part of Kalochori. As a countermeasure, in 1969 the government built the first embankment to protect the area from the sea. Unfortunately, this construction has frequently suffered severe failures. All the efforts aiming to reinforce the embankment were in vein. The first collapse occurred four years after its construction and a new construction was built in 1976. However, before the end of the 1970s, it was completely destroyed. The need for the protection of the coastal area led the government to take more measures against the hazard and thus in 1980 a larger embankment (the one that still stands today) was constructed that was considered to be more suitable to face the wave loadings and the subsidence deformations. Unfortunately this man-made sea-barrier isolated an area of land, turning it into a lagoon. In order to avoid new flood phenomena, pumping stations were widely used during wet seasons. The continuous subsidence has caused significant damage, as for example water well pipe protrusion, farmland flooding and loss of infrastructures (Fig. 3). Even today, extreme weather events cause extensive surface flooding, as the plumbing stations are incapable to drain the coastal area located below sea level.

At this point it should be noted that at the entire study area neither surface ruptures nor differential displacements have been reported, despite the intensity of the land subsidence phenomena. This phenomenon is unique, at least in Greece, and it can only be attributed to the absence of faults intersecting the top layers within the narrow limits of the study area. It is a fact that the faults' offset create intense variations at the thickness of the compressible formations leading to the manifestation of differential displacements in case of ground water drawdown (Loupasakis et al., 2014).

The aforementioned hazardous facts have invoked a rising interest among the scientists to elucidate the driver mechanism, and various

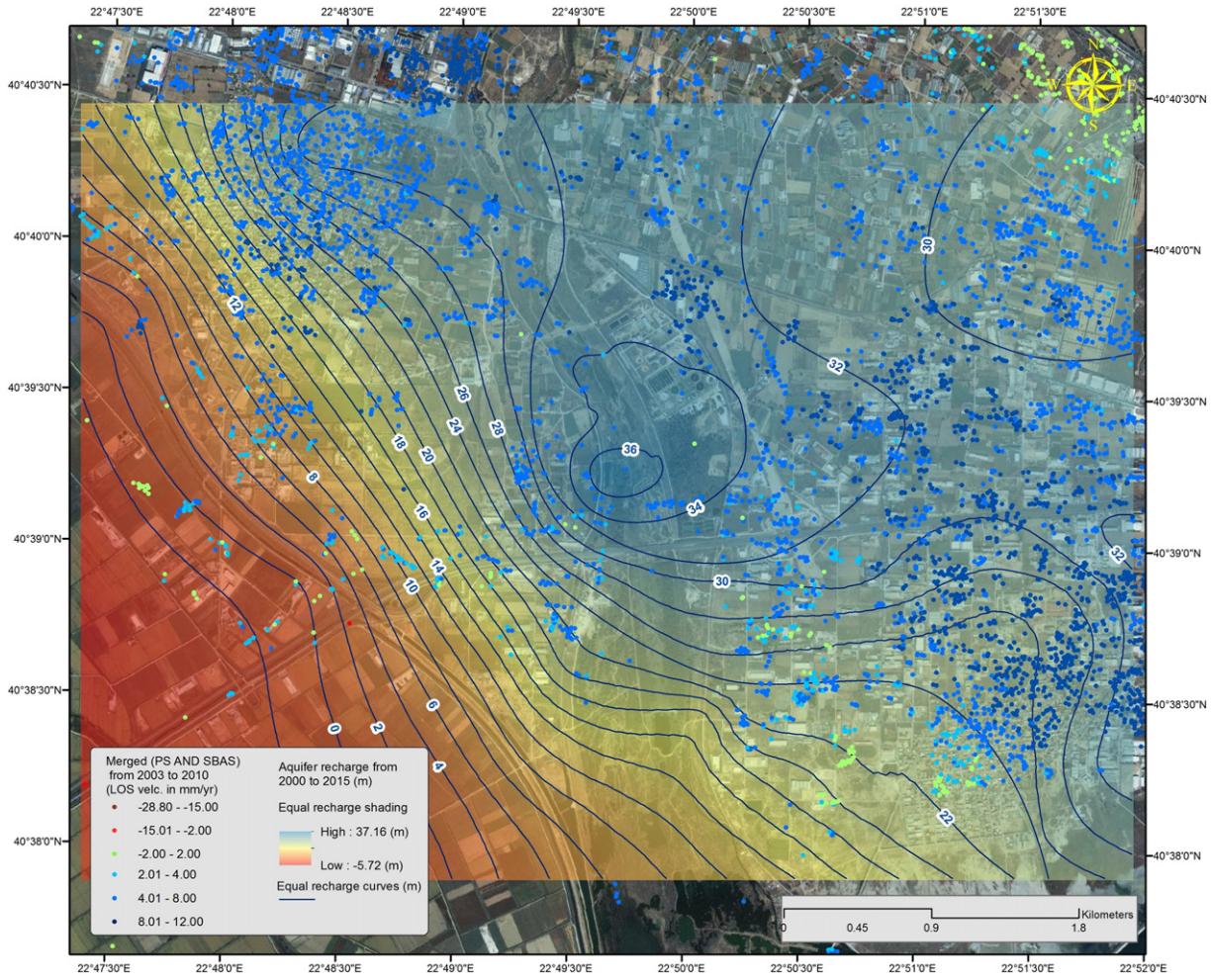

Fig. 5. Image presenting the groundwater recharge (in m) between June 2000 and June 2015. The dots are SAR data indicating displacements along LOS in mm/year (2003–2010). Positive values of the aquifers recharge contour indicate uplifting of the ground water level.

ideas were discussed about the nature of the subsidence. The Kalochori and Sindos sites have been studied using ground truth, levelling, GPS and InSAR techniques (e.g. Costantini et al., 2016; Doukas et al., 2004; Mouratidis et al., 2009; Psimoulis et al., 2007; Raspini et al., 2014; Raucoules et al., 2008; Stiros, 2001). The general consensus amongst scientists was that the detected subsidence is mainly attributed to the excessive ground water pumping (Andronopoulos et al., 1990; Hatzinakos et al., 1990; Loupasakis and Rozos, 2009; Raspini et al., 2014; Rozos and Hatzinakos, 1993) while additional deformations due to natural compaction of loose Quaternary deposits cannot be excluded (Psimoulis et al., 2007). Several other scenarios have also been proposed. For example, Doukakis (2005) linked the deformation to the effects of the caused coastal erosion and sea level rise due to climate change. A more geotechnical approach included coastal flowing sand phenomenon and the consolidation of the loose silty-clay deposits (Dimopoulos, 2005). Stiros (2001) attributed the detected subsidence to the cumulative effect of a piezometric surface decline, the oxidation of peat soils in the vadose zone, the synsedimentary deformation of the delta, the consolidation of the deeper sediments (as a result of the upper strata loading) and the consolidation of near surface sediments.

3. Geological and hydrogeological facts of the study area

3.1. Geological and hydrogeological setting

The wider, Sindos and Kalochori areas founded over Quaternary deposits. Sands, clays and silty clays are the main contents of these deposits (Hatzinakos et al., 1990; Rozos et al., 2000) (Fig. 4). North and northeastern of the study area there are sandstones, and red clays, contents of the Neogene basement outcrop. Their depth underneath Kalochori is known to be at 700 m (Demiris, 1988).

The upper strata of the Quaternary formations, down to a depth of at least 200 m, can be divided in three horizons. According to Rozos et al. (2000) the order is: a) a sandy horizon, b) an impermeable silty clay layer and c) alternating layers of coarse and fine sediments. The upper horizon consists of yellow-brown fine to medium grain sands with silty bands intercalations. At a depth of 25 to 35 m, at the Kalochori region, and a few meters shallower at the wider Sindos area, lies the underlying impermeable silty clays horizon. Finally, the deeper horizon consists of alternating brown sands and black-grey silty sands (Loupasakis and Rozos, 2010). The uppermost sandy horizon hosts a shallow unconfined aquifer. This shallow aquifer contains very poor quality water, has an upper level of 1.3 m and a lower level of 3 m. The thickness of this underground water body is 10 to 15 m. Below the silty clay impermeable horizon, lies an artesian aquifers system with good water quality, hosted inside the alternating layers.

3.2. History of the water level changes

Back in the 1950s at the study area, the lower aquifer system was artesian. On the contrary, that was not the case for the next decades, which were characterized by a continuous lowering of the piezometric surface of the deeper aquifer (Raspini et al., 2014). At the wider area of Kalochori and Sindos more than 400 deep wells were extracted (Soulios, 1999) and except those of the Water Supply Company, the vast majority of the rest were unauthorized high consumption industrial drills. The lowering of the piezometric surface was more intense since the early 1980s where many deep drills had already been active and the decrease of the confined aquifer's level was lowered down to 40 m (Andronopoulos et al., 1990). On the contrary, all this years' piezometry of the upper unconfined aquifer has not been subjected to any change. This is due to the fact that the water quality of the upper aquifer is low leading to its light exploitation. Furthermore the intense cultivation of rice at the majority of the farmlands of the area kept this aquifer to a continuous recharge.

Table 1
ERS dataset that was used in the time-series analysis.

Dates	Perp. baseline(m)	Δt (days)
12-Nov.-92	127 m	−933
19-Aug.-93	−318 m	−653
28-Oct.-93	593 m	−583
03-Jun.-95	0 m	0
13-Aug.-95	100 m	71
30-Dec.-95	445 m	210
31-Dec.-95	199 m	211
09-Mar.-96	527 m	280
14-Apr.-96	201 m	316
18-May-96	157 m	350
19-May-96	82 m	351
01-Sep.-96	−67 m	456
06-Oct.-96	−506 m	491
15-Dec.-96	−369 m	561
04-May-97	−310 m	701
08-Jun.-97	−15 m	736
13-Jul.-97	−361 m	771
17-Aug.-97	−158 m	806
21-Sep.-97	−110 m	841
30-Nov.-97	129 m	911
04-Jan.-98	−261 m	946
19-Apr.-98	206 m	1051
28-Jun.-98	116 m	1121
02-Aug.-98	221 m	1156
06-Sep.-98	−831 m	1191
28-Feb.-99	47 m	1366
13-Jun.-99	48 m	1471
18-Jul.-99	340 m	1506
22-Aug.-99	−525 m	1541
26-Sep.-99	481 m	1576

In the mid-1980s a temporary groundwater level recovery of 5 to 15 m occurred since the Water Company had stopped pumping, aiming to control land subsidence phenomena. At the late 1990s the increasing water consumption, by the industries, led the underground water level to be at its maximum depth of 35–40 m below ground level (Raspini et al., 2014, Soulios, 1999). Interestingly enough, in 2012 the aquifer appeared to be partially recovered and the water level was located from +1 above to 8 m below ground level. The spatial distribution of

Table 2
ENVISAT dataset that was used for the time-series analysis.

Dates	Perp. baseline(m)	Δt (days)
9-Mar.-03	−404	−2065
22-Jun.-03	−232	−1960
11-Jul.-04	−231	−1575
24-Oct.-04	394	−1470
6-Feb.-05	−474	−1365
13-Mar.-05	366	−1330
17-Apr.-05	156	−1295
22-May-05	−126	−1260
4-Sep.-05	639	−1155
26-Feb.-06	−317	−980
11-Jun.-06	−314	−875
16-Jul.-06	793	−840
11-Feb.-07	−298	−630
5-Aug.-07	−158	−455
6-Apr.-08	221	−210
20-Jul.-08	48	−105
2-Nov.-08	0	0
11-Jan.-09	−49	70
15-Feb.-09	−79	105
26-Apr.-09	−155	175
31-May-09	31	210
13-Sep.-09	342	315
22-Nov.-09	209	385
27-Dec.-09	−379	420
7-Mar.-10	−213	490
11-Apr.-10	136	525
20-Jun.-10	−2	595

the ground water level recovery between 2000 and 2015 is presented in the form of equal recharge contour lines in Fig. 5. It is clear that at 2015 the water level appears to be recovering; throughout the entire study area. The aforementioned recovery is highly connected with the economic crisis that has led most of the industries to shut down, reducing radically the water consumption.

4. Data processing and adopted methods of Remote Sensing

4.1. Software

The open source software StaMPS (Stanford Method for Persistent Scatterers) (Hooper, 2006; Hooper et al., 2007) was used. For time series studies, the use of StaMPS, requires additional software, prior to the mass processing. For this purpose ROI_PAC (Repeat Orbit Interferometry Package), developed by California Institute of Technology and Jet Propulsion Laboratory (NASA), is used for the focusing of the raw radar data and DORIS (Delft object-oriented radar Interferometric software) for the Interferograms generation.

4.2. Input data & methods adopted

4.2.1. Input data

SAR data provided by ESA (European space Agency) from the satellites ERS 1/2 & Envisat and for the time spans 1992 to 2000 and 2003 to 2010 respectively are analysed for the estimation of the surface deformation. The initial dataset consists of 46 Images (level_0) for ERS missions and 37 (level_0) for ENVISAT, both from the track 279 from the descending mode. The final used dataset is presented in Tables 1 and 2. The SRTM DEM was used for the topographic correction. For Orbital corrections the information from the Department of Earth Observation and space systems (DEOS) of the Delft University of Technology and VOR data from ESA were adopted. Moreover, ground truth data from field surveys and hydrogeological data from the water supply and Sewerage Company of Thessaloniki are taken into account for the validation and interpretation of the detected signal.

4.2.2. Interferometry techniques employed

Differential Interferograms are the starting basis for the SAR time series analysis. For the generation of an Interferogram, the level_0 products (raw satellite data) are focused for the creation of a Single Look Complex Image (SLC). Cross-correlation techniques are then used to co-register two SLC images, acquired over the same area of interest at different times, and estimate the coherence of the Interferometric phase. As time goes by, an area on land is being subjected to minor or major changes on the surface. The less the changes, the higher the coherence. Thus, in urban areas high coherence is expected, whereas in agricultural lands or wetlands (i.e. in areas where there are frequent surface changes) low coherence is expected.

After the co-registration the phases of the two SLC images are subtracted and an Interferogram is formed. Corrections are then applied to account for the contribution of the earth's curvature and the topography using an a priori known Digital Elevation Model. The result is a wrapped Differential Interferogram (DInSAR) that depicts the crustal deformation which occurred between the two passes of the satellite (Fig. 6). A critical subsequent step is the unwrapping of the Interferogram where the phase differences are translated to absolute distances from the satellite (in the Line of Sight). Throughout the whole procedure, spatial filtering is an important factor to increase Signal-to-Noise levels. For further information on SAR Interferometry the reader should

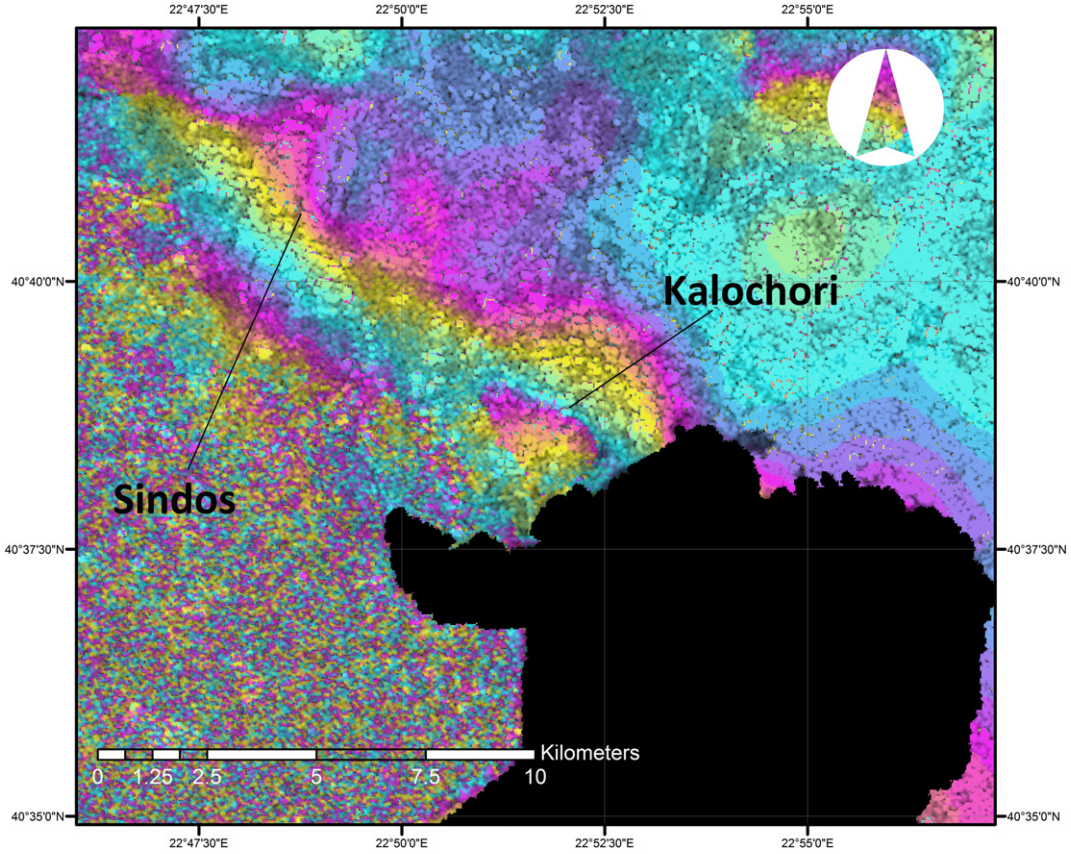

Fig. 6. Differential Interferogram of the pair of the acquisitions: 17 September 1995 and 1 September 1996. Areas with random colours (at the south western part) are areas of low coherence. This is due to the agricultural lands of Thessaloniki Plain. The areas of Kalochori and Sindos are located in detected deforming areas (areas with non-random colours that form the "fringes": repeated colour cycles) as it can be seen on this phase map. (For interpretation of the references to colour in this figure legend, the reader is referred to the web version of this article.)

refer to Dixon (1994); Massonnet and Feigl (1998); Massonnet (1997); Zebker and Goldstein (1986).

The Permanent Scatterers (PS) Interferometry (Ferretti et al., 2000, 2001) creates a network of SLC pairs in which all of the SLC slaves are connected with a unique SLC image (master) selected by the analyst. The selection lies on the basis of maximising the expected ensemble coherence considering the perpendicular, Doppler and temporal baselines (Hooper et al., 2007). The pairs are the differential Interferograms to be formed. The procedure searches in the stack of the Interferograms for PS candidates. The latter are specific points in the study area that pass the criteria of stable radiometric characteristics throughout time. These points, strongly correlated in time and space, are the points on the surface at which ground velocities are going to be estimated. Most of the times, PS can be urban constructions, metallic fences, corner reflectors etc. Areas with frequent surface changes throughout the time of the study are areas with low coherence. This is due the fact that there is a different amount of micro-wave backscattering to the satellite at each acquisition. For the points of low coherence there is no information on the deformation and they are not considered as PS. With the PS technique there is the ability to have precise mm-scale measurements of unique objectives-targets on the ground.

The method of Small Baseline Subset (SBAS) (Berardino et al., 2002) has the aim to minimize the geometric decorrelation using small baselines (the vertical distance between the two satellite trajectories).

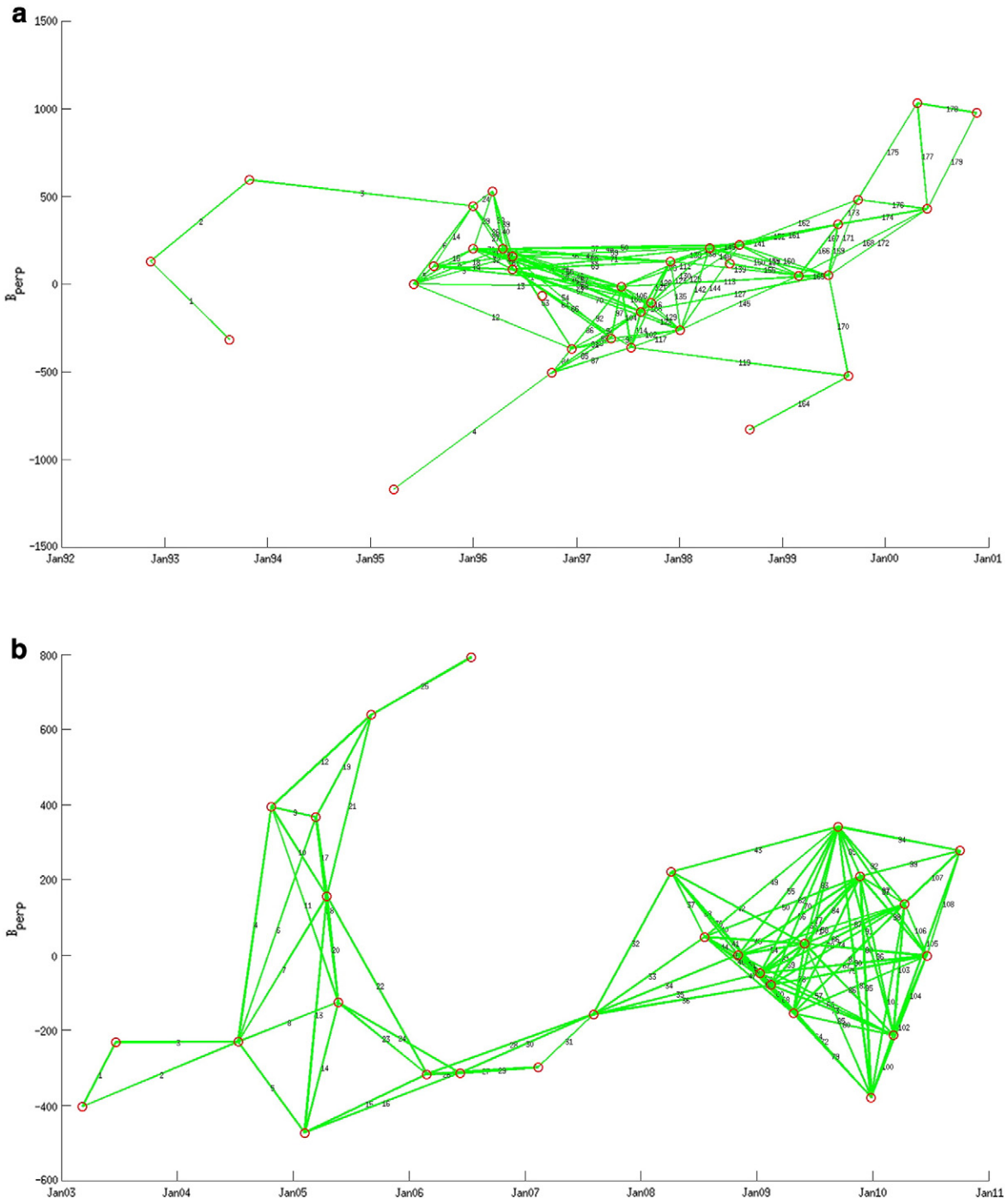

Fig. 7. a Connection graph showing the Differential Interferograms created for the SBAS technique for the ERS dataset b Connection graph showing the SLC network created for the SBAS technique for the ENVISAT dataset.

A connection graph of SLC pairs (DInSAR's) is created based on the choice of the maximum allowed baselines and the maximum allowed temporal separation. The technique minimizes the effect of limited coherency. Although not so accurate like PS, the advantage is that SBAS gives a broader sense of the deforming surface by offering more pixel measurements.

SBAS and PS are different SAR time-series methods to measure ground deformation. In general, we would say that for the study of tectonic movements SBAS appears to be a more suitable choice because it gives the sense of the deformation of larger areas of terrain by offering more point coverage. On the other hand, for high accuracy measurements in the urban environment PS is more reliable. The StaMPS algorithm offers the opportunity to combine these two and have a merged final result.

5. Application results and discussion

Correlating the deformation history, as presented through the SAR time-series analysis, with hydrogeological data, a high connection was found. The connection graphs, showing the created SLC image pairs during the mass processing, for both datasets, are presented in Fig. 7a, b. For the time series analysis the reference point was set at an area where there is absence of deformation (at the center of the city of Thessaloniki). Figs. 8 and 9 show the deformation velocities for the period 1992–2000 and 2003 to 2010, respectively. As it can be seen the deformation patterns of Figs. 8 and 9 present opposite trends. From 1992 to 2000 a subsiding surface was revealed (more than 20 mm/year) and from 2003 to 2010 there is uplift (up to 12 mm/year). When it comes to the spatial amount of the uplifting pattern, Kalochori is having larger values of uplift, when compared to Sindos.

A technical validation of the results stems from the fact that these very interesting ground velocity estimations were measured by all the three techniques applied (PS, SBAS, Merged result). In order to further validate and interpret these results, ground truth data were exploited.

In Fig. 5 the velocities derived from the SAR analysis are compared with the ground water level recovery between 2000 and 2015, presented in the form of equal recharge contour lines. Positive contour values indicate recharge and, there is a clear relation of the uplifting trend detected by the SAR analysis with the spatial distribution of the aquifers recovery. There is not a straight correlation between the maximum water level recharge values and the maximum amount of uplift throughout the whole area. That is due to the fact that except the

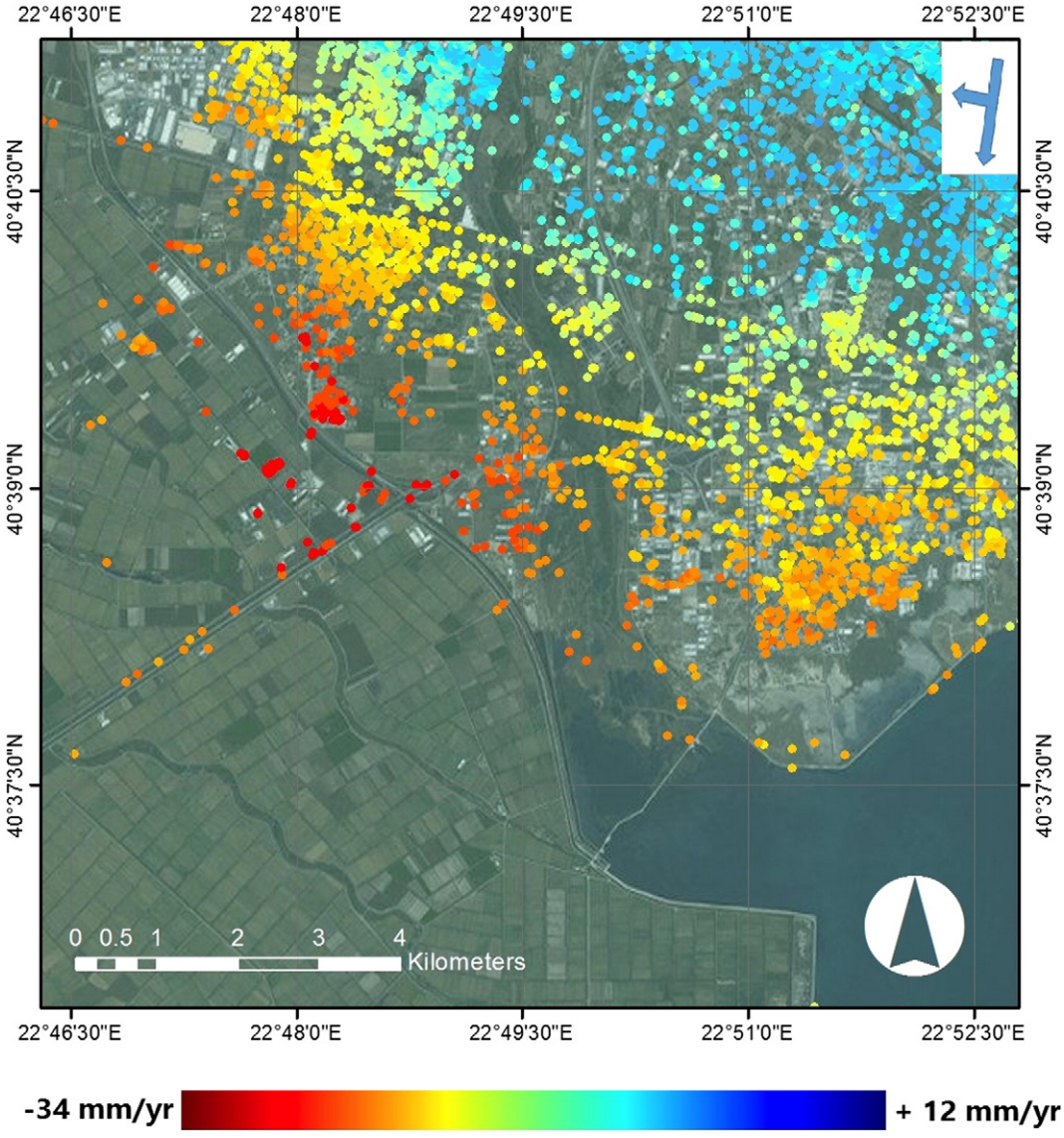

Fig. 8. Velocities from 1993 to 2000 as derived by the analysis of ERS 1 & 2 data. During this time period the study area was subsiding with a rate of 20 mm/year. The large arrow depicted in the inset in the upper right, shows the direction of the descending path and vertical smaller arrow shows the line of sight direction of the satellite.

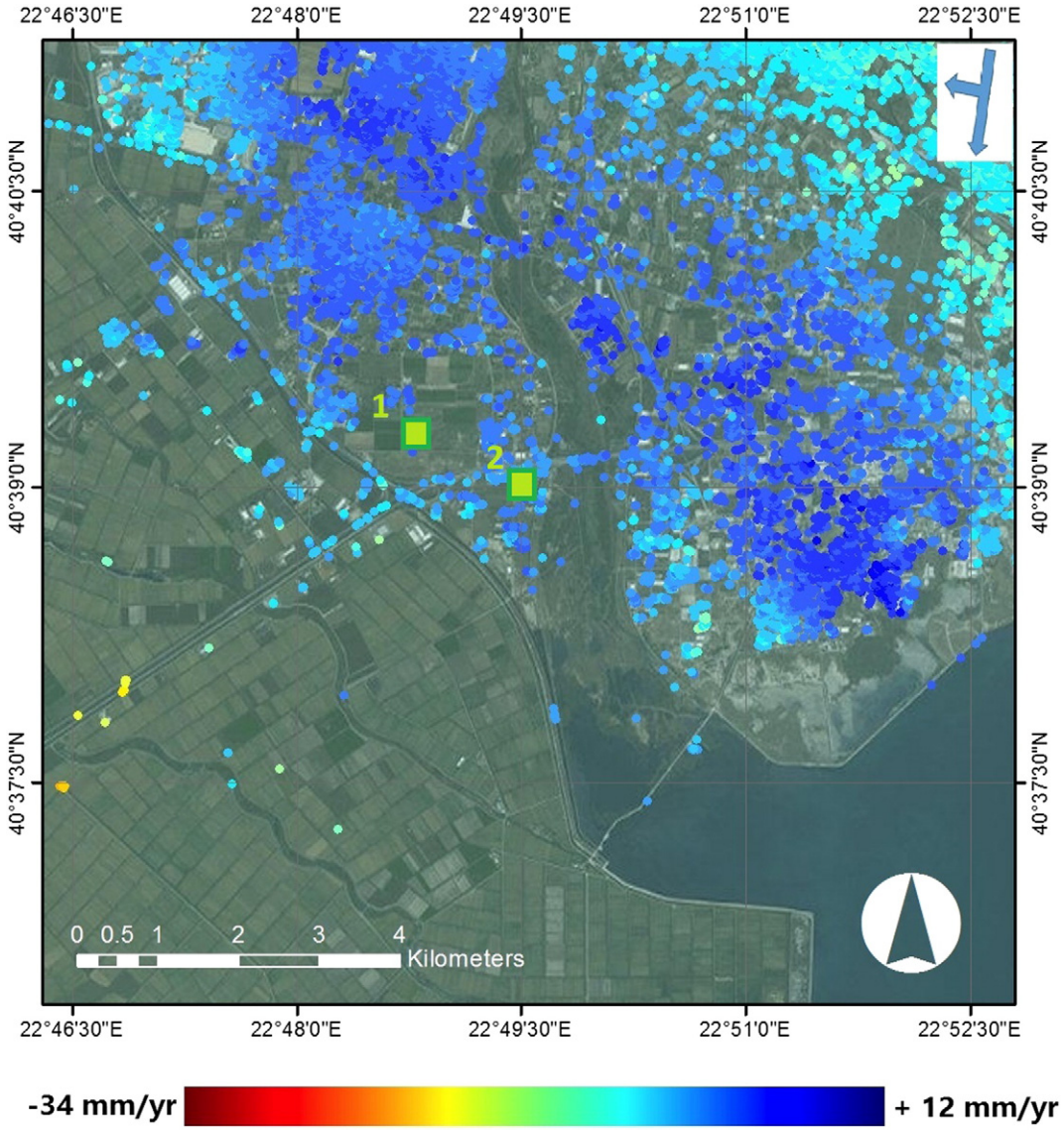

Fig. 9. Velocities from 2003 to 2010 from the analysis of ENVISAT data. The area is subjected to uplift. The uplifting rates are up to 12 mm/year. The green rectangles (1 and 2) denote the location of the drills whose data were used for designing the curves of Fig. 10 and Fig. 11. The large arrow depicted in the inset in the upper right, shows the direction of the descending path and vertical smaller arrow shows the line of sight direction of the satellite. (For interpretation of the references to colour in this figure legend, the reader is referred to the web version of this article.)

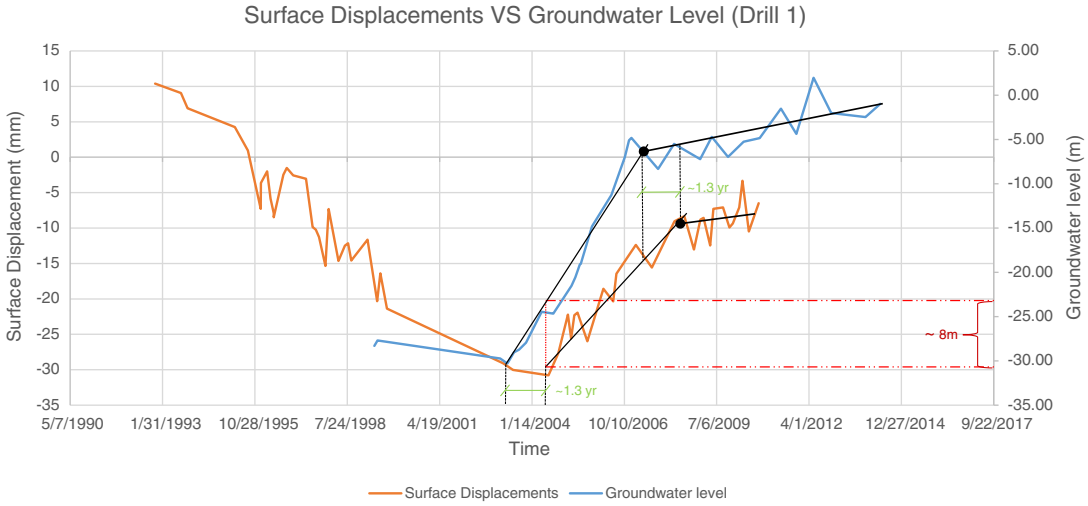

Fig. 10. Graph comparing the ground water level variations at Drill 1 with the surface deformation time series at a nearby data point produced by the SAR analysis.

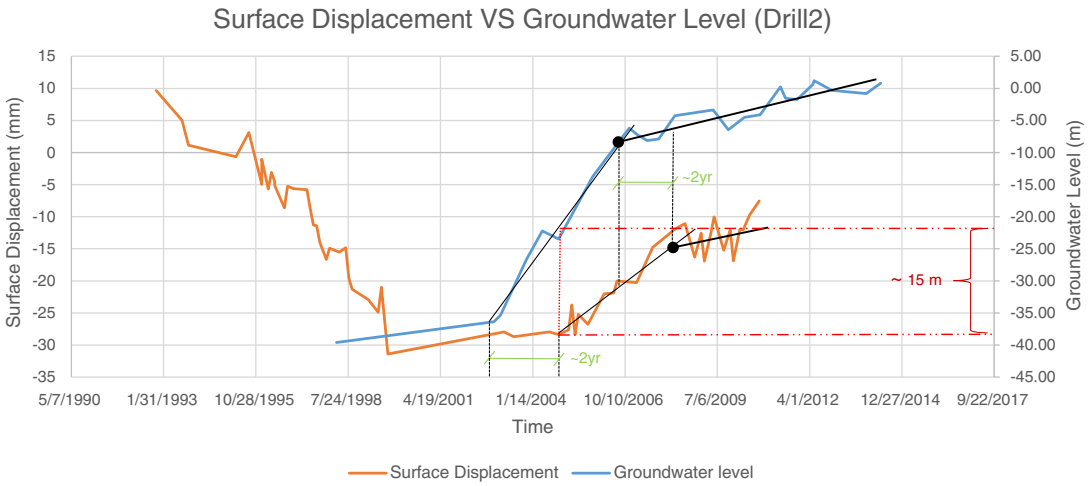

Fig. 11. Graph comparing the ground water level variations at Drill 2 with the surface deformation time series at a nearby data point produced by the SAR analysis.

ground water level, the different geotechnical characteristics and the stratigraphy variations affect the uplift ratio.

In the same context, a more in-depth analysis was conducted by designing the graphs of Figs. 10 and 11. The two-decade of deformation history were plotted together with the ground water level measurements at, neighbouring time series velocity points and drills (green rectangles in Fig. 9). When looking at the general trend of both graphs (Figs. 10 and 11), the surface deformation is presenting three distinctive trends. The first one (negative slope) is expressing the first period where subsidence was occurring. The second one (positive slope) after 2000 presents the uplifting trend. And finally the third one (positive slope) after 2007 denotes a smoother uplifting trend. The correlation of the subsiding trend with the aquifer water level measurements makes clear that the changes of the aquifer level is followed by a proportional response detected at the surface.

It is really important to point that there is a sufficient time-lag between the recharge initiation and the responding uplift at the ground surface. As presented in Figs. 10 and 11 this time-lag is approximately 1.3 to 2 years and it can be completely justified by the consolidation theory (Terzaghi, 1943). Specifically, the swelling index, Cs, representing the increase of the void ratio, e, as a function of the reduction of effective stress, σ_{ef}, is 5 to 10 times smaller than the compression index, Cc, representing the reduction of the void ratio, e, as a function of the increment of effective stress. Thus, soil formations swell 5 to 10 times less when a load is removed, than compress when the same amount of load is applied. That means that in order to get measurable swelling indications the reduction of the effective loads has to be intensive. This is why, at the typical oedometer test, maximum loading is gradually applied in more than five stages and unloading in just one stage, by removing all loads at once.

In the case of aquifer recharge the unloading is applied by the increment of the pore pressure, decreasing proportionally the effective stresses. As it can be seen at the graphs of Figs. 10 and 11, at the current case study in order to get some swelling indications at the surface the ground water level had to get uplifted for at least 8 to 15 m, succeeding a proportional reduction of the effective stresses equal to 100 kN/m^2. This 8 to 15 m recharge took approximately 1.3 to 2 years to take place, justifying the time-lag.

6. Conclusions

Time-series surface deformation analysis is carried out for the areas of Sindos and Kalochori and for the interpretation and validation ground truth based data were used. Sindos and Kalochori (parts of the Delta municipality) are both industrial suburbs of the city of Thessaloniki. ERS and ENVISAT images covering the study area, from 1993 to 2010, have been analyzed by generating more than 250 Interferograms.

For the wider study area various studies have already highlighted a subsiding trend, attributed by most of the researchers to the overexploitation of the aquifers. SAR Interferometry is one of the tools widely used up to now for the detection and investigation of subsidence phenomena occurring from 1993 to 2000. In this study, the previously detected subsidence is validated, whereas now an uplifting trend is highlighted for the same area from 2003 to 2010.

The detected deformation rebound of 2003 to 2010, occurring in agreement to the recharge of the aquifers, proves that the ground water overexploitation was the driving mechanism of the subsidence phenomena all these decades. Even though the parallel activity of other phenomena, such as natural compaction and soil oxidation cannot be excluded, the detected rebound leaves no room for other speculations concerning the dominant driving mechanism. It is clear that even though other deformation mechanisms might be occurring, their contribution was neglectable and unable to restrain the surface rebound that took place the last decade. The most intriguing result of the validation procedure was the detected 1.3 to 2 years long time-lag between the recharge initiation and the responding uplift of the ground surface. This fact is recorded and reported for the first time and it is clearly justified by the consolidation theory.

The physical interpretation of the observed uplift phenomenon is linked to the fact that at the beginning of the 20th century the economical status at the industrial areas of Kalochori and Sindos changed. Several water consuming industries of the secondary economic sector, such as textiles, clothing and skin processing industries, shut down and their place was taken by companies of the tertiary economic sector, such as logistics and import–export companies. This change on the economic status of the area together with the national economic collapse led to the gradual reduction of the ground water consumption and as a result to the aquifers recharge.

Nevertheless due to the fact that the study areas remain an important industrial and traffic in transit centre for southeastern Balkans, the recommendations derived from the current work, clearly support the need for a comprehensive water management strategy that would include detailed hydrogeological studies in order to avoid the regeneration of the hazard of the past in the future. The measures to be taken and the strategic plan, rely within the authorization of the Greek government.

Acknowledgments

We would like to thank Roy J. Shlemon and one anonymous reviewer for their fruitful comments. We acknowledge the European Space

Agency (ESA) for the SAR data contribution (ERS and ENVISAT) in the framework of ESA-GREECE AO project 14890D/11-2003/72. Hydrogeological data are courtesy of the Water Supply and Sewerage Company of Thessaloniki (EYATH). We thank Xanthos Papanikolaou and Demitris Anastasiou from Dionysos Satellite Observatory. The Interferometric processing was performed using the Doris software package developed by the Delft Institute of Earth Observation and Space Systems (DEOS), Delft University of Technology also ROI_PAC software for raw data focusing and StaMPS software for the time-series analysis. This work was partially funded by a) the European Union 7th Framework Programme (FP7-REGPOT-2012-2013-1), in the framework of the project BEYOND "Building a Centre of Excellence for EO-based monitoring of Natural Disasters", G. A. 316210 and b) by the European Union (European Social Fund—ESF) (MIS377335) and Greek national funds through the Operational Program "Education and Lifelong Learning" of the National Strategic Reference Framework (NSRF)—Research Funding Program: Thales - Investing in knowledge society through the European Social Fund (MIS377335 Prof A. Kiratzi coordinator).

References

Amelung, F., Galloway, D.L., Bell, J.W., Zbeker, H.A., Laczniak, R.J., 1999. Sensing the ups and downs of Las Vegas: InSAR reveals structural control of land subsidence and aquifer-system deformation. Geology 27 (6), 483–486.

Andronopoulos, V., Rozos, D., Hadzinakos, J., 1990. Geotechnical study of ground settlement in the Kalochori area, Thessaloniki District. Unpublished Report IGME. E6319, p. 45.

Bell, J.W., Amelung, F.A., Ferretti, A., Bianchi, M., Novali, F., 2008. Permanent scatterer InSAR reveals seasonal and long-term aquifer-system response to groundwater pumping and artificial recharge. Water Resour. Res. 44 (2), 2407–2425.

Berardino, P., Fornaro, G., Lanari, R., Sansosti, E., 2002. A new algorithm for surface deformation monitoring based on small baseline differential SAR interferograms. IEEE Trans. Geosci. Remote Sens. 40, 2375–2383.

Chen, C., Hu, J., Lu, C., Lee, J., Chan, Y., 2007. Thirty-year land elevation change from subsidence to uplift following the termination of groundwater pumping and its geological implications in the Metropolitan Taipei Basin, Northern Taiwan. Eng. Geol. 95, 30–47.

Costantini, F., Mouratidis, A., Schiavon, G., Sarti, F., 2016. Advanced InSAR techniques for deformation studies and for simulating the PS-assisted calibration procedure of Sentinel-1 data: case study from Thessaloniki (Greece), based on the Envisat/ASAR archive. Int. J. Remote Sens. 37 (4), 729–744. http://dx.doi.org/10.1080/01431161.2015.1134846.

Demiris, K., 1988. Geological settings and their influence on the development of the areas on the west of Thessaloniki. Proceedings of the Symposium on the Technical Problems Affecting the Areas on the West of Thessaloniki. Technical Chamber of Greece, Thessaloniki.

Dimopoulos, G., 2005. Investigation of the conditions generating soil settlements in Sindos–Kalochori area of Thessaloniki. Proceedings of the 7th Hellenic Hydrogeological Conference and 2nd MEM Workshop on Fissured Rocks Hydrogeology, Athens. Hellenic Committee of Hydrogeology, pp. 135–146.

Dixon, T.H., 1994. SAR interferometry and surface change detection. Report of a Workshop, Boulder, Colorado, USA.

Doukakis, E., 2005. Coastal red spots along the western Thermaikos gulf. Proceedings of the 9th International Conference on Environmental Science and Technology. University of Aegean, Rhodes, Greece, pp. A334–A339.

Doukas, I.D., Ifadis, I.M., Savvaidis, P., 2004. Monitoring and analysis of ground subsidence due to water pumping. FIG Working Week, Athens, Greece, May 22–27.

Ferretti, A., Prati, C., Rocca, F., 2000. Nonlinear subsidence rate estimation using permanent scatterers in differential SAR interferometry. IEEE Trans. Geosci. Remote Sens. 38, 2202–2212.

Ferretti, A., Prati, C., Rocca, F., 2001. Permanent scatterers in SAR interferometry. IEEE Trans. Geosci. Remote Sens. 39, 8–20.

Fruneau, B., Sarti, F., 2000. Detection of ground subsidence in the city of Paris using radar interferometry: isolation of deformation from atmospheric artifacts using correlation. Geophys. Res. Lett. 27, 3981–3984.

Galloway, D.L., Hoffmann, J., 2007. The application of satellite differential SAR interferometry-derived ground displacements in hydrogeology. Hydrogeol. J. 15 (1), 133–154. http://dx.doi.org/10.1007/s10040-006-0121-5.

Galloway, D.L., Hudnut, K.W., Ingebritsen, S.E., Phillips, S.P., Peltzer, G., Rogez, F., Rosen, P.A., 1998. Detection of aquifer system compaction and land subsidence using interferometric synthetic aperture radar, Antelope Valley, Mojave Desert, California. Water Resour. Res. 34, 2573–2585.

Hatzinakos, I., Rozos, D., Apostolidis, E., 1990. Engineering geological mapping and related geotechnical problems in the wider industrial area of Thessaloniki, Greece. In: PRICE, D. (Ed.), Proceedings of Sixth International IAEG Congress, Amsterdam, Balkema, pp. 127–134.

Hooper, A., 2006. Persistent Scatterer Radar Interferometry for Crustal Deformation Studies and Modeling of Volcanic Deformation PhD thesis Stanford University.

Hooper, A., Segall, P., Zebker, H., 2007. Persistent scatterer interferometric synthetic aperture radar for crustal deformation analysis, with application to Volcán Alcedo, Galápagos. J. Geophys. Res. 112, B07407. http://dx.doi.org/10.1029/2006JB004763.

IGME - Institute of Geological and Mineralogical Exploration (1978) Geological Map of Greece, Scale 1:50.000, Thessaloniki Sheets, IGME Athens.

Ikehara, M.E., Phillips, S.P., 1994. Determination of land subsidence related to groundwater-level declines using Global Positioning System and leveling surveys in Antelope Valley, Los Angeles and Kern counties, California, 1992. U.S. Geol. Surv. Water Resour. Invest. Rep. 94–4184.

Ishitsuka, K., Fukushima, Y., Tsuji, T., Yamada, Y., Matsuoka, T., Giao, P.H., 2014. Natural surface rebound of the Bangkok plain and aquifer characterization by persistent scatterer interferometry. Geochem. Geophys. Geosyst. 15, 965–974. http://dx.doi.org/10.1002/2013GC005154.

Kapsimalis, V., Poulos, S.E., Karageorgis, A.P., Pavlakis, P., Collins, M.B., 2005. Recent evolution of a Mediterranean deltaic coastal zone: human impacts on the Inner Thermaikos Gulf, NW Aegean Sea. J. Geol. Soc. Lond. 162, 1–12.

Kiratzi, A., 2014. Mechanisms of earthquakes in Aegean. Encyclopedia of Earthquake Engineering, 382074.

Le Mouelic, S., Raucoules, D., Carnec, C., King, C., 2002. A ground uplift in the city of Paris (France) Detected by Atellite Radar Interferometry. Geophys. Res. Lett. 29, 1853. http://dx.doi.org/10.1029/2002GL015630.

Loupasakis, C., Rozos, D., 2009. Land subsidence induced by water pumping in Kalochori village (North Greece) - simulation of the phenomenon by means of the finite element method. Q. J. Eng. Geol. Hydrogeol., Geol. Soc. Lond. 42 (3), 369–382.

Loupasakis, C., Rozos, D., 2010. Land subsidence induced by the overexploitation of the aquifers in Kalochori village – new approach by means of the computational geotechnical engineering. Proceedings of the 12th International Congress of the Geological Society of Greece. Bulletin of the Geological Society of Greece XLIII, pp. 1219–1229 No 3.

Loupasakis, C., Agelitsa, B., Rozos, D., Spanou, N., 2014. Mining geohazards—land subsidence caused by the dewatering of opencast coal mines: the case study of the Amyntaio coal mine, Florina, Greece. Natural Hazards 70. Springer, pp. 675–691. http://dx.doi.org/10.1007/s11069-013-0837-1.

Massonnet, D., 1997. Satellite radar interferometry. Sci. Am. 276 (2), 46–53.

Massonnet, D., Feigl, K., 1998. Radar interferometry and its application to changes in the Earth's surface. Rev. Geophys. 36, 441–500.

Massonnet, D., Rossi, M., Carmona, C., Adragna, F., Peltzer, G., Feigl, K., Rabaute, T., 1993. The displacement field of the Landers earthquake mapped by radar interferometry. Nature 364, 138–142.

Mouratidis, A., Briole, P., Ilieva, M., Astaras, T., Rolandone, F., Baccouche, M., 2009. Subsidence and deformation phenomena in the vicinity of Thessaloniki (N. Greece) monitored by Envisat/ASAR interferometry. Proceedings of Fringe 2009, Frascati, Italy.

Petsas, P., 1978. Pella, Alexander the Great's Capital. 1978. Institute for Balkan Studies, Thessaloniki (164 pp.).

Phien-wej, N., Giao, P.H., Nutalaya, P., 2006. Land subsidence in Bangkok, Thailand. Eng. Geol. 82 (4), 187–201.

Psimoulis, P., Ghilardi, M., Fouache, E., Stiros, S., 2007. Subsidence and evolution of the Thessaloniki plain, Greece, based on historical leveling and GPS data. Eng. Geol. 90, 55–70.

Raspini, F., Loupasakis, C., Rozos, D., Moretti, S., 2013. Advanced interpretation of land subsidence by validating multi-interferometric SAR data: the case study of the Anthemountas basin (Northern Greece). Nat. Hazards Earth Syst. Sci. 13 (10), 2425–2440.

Raspini, F., Loupasakis, C., Rozos, D., Adam, N., Moretti, S., 2014. Ground subsidence phenomena in the Delta municipality region (Northern Greece): Geotechnical modeling and validation with Persistent Scatterer Interferometry. Int. J. Appl. Earth Obs. Geoinf. 28, 78–89.

Raucoules, D., Parcharidis, I., Feurer, D., Novali, F., Ferretti, A., Carnec, C., Lagios, E., Sakkas, V., Le Mouelic, S., Cooksley, G., Hosford, S., 2008. Ground deformation detection of the greater area of Thessaloniki (Northern Greece) using radar interferometry techniques. Nat. Hazards Earth Syst. Sci. 8, 779–788.

Rozos, D., Hatzinakos, I., 1993. Geological conditions and geomechanical behaviour of the neogene sediments in the area west of Thessaloniki (Greece). In: Anagnostopoulos, et al. (Eds.), Proceedings of International Symposium on Geotechnical Engineering of Hard Soils – Soft Rocks, Greece 1. Balkema, Rotterdam, pp. 269–274.

Rozos, D., Apostolidis, E., Christaras, B., 2000. Engineering – geological map of Thessaloniki wider area. Proceedings of National meeting on protection of Thessaloniki from Natural Hazards, pp. 46–53.

Sivignon, M., 1987. In: Bethemont, J., Villain-Gandossi, C. (Eds.), La mise en valeur du delta de l'Axios.

Soulios, G., 1999. Research for the development of the aquifers in the low lands on the west of Thessaloniki for the interests of the Water Company of Thessaloniki. Research Committee Technical Report. Aristotle University of Thessaloniki, p. 99.

Stiros, S., 2001. Subsidence of the Thessaloniki (northern Greece) coastal plain, 1960–1999. Eng. Geol. 61 (4), 243–256.

Svigkas, N., Papoutsis, I., Loupasakis, K., Kontoes, H., Kiratzi, A., 2015. Geo-hazard monitoring in Northern Greece using InSAR techniques: the case Study of Thessaloniki, (Abstract ID33). 9th International Workshop Fringe 2015 "Advances in the Science and Applications of SAR Interferometry and Sentinel-1 InSAR", ESA-ESRIN, Frascati, Italy 23–27 March 2015.

Syrides, G.E., 1990. Lithostratigraphic, biostratigraphic and palaeogeographic study of the Neogene–Quaternary sedimentary deposits of Chalkidiki Peninsula, Macedonia, Greece Ph.D. thesis Aristotle University of Thessaloniki 243 pp. (in Greek).

Taniguchi, M., Shimada, J., Fukuda, Y., Yaman, M., Onodera, S., Kaneko, S., Yoshikoshi, A., 2009. Anthropogenic effects on the subsurfacethermal and ground water

environments in Osaka, Japan and Bangkok, Thailand. Sci. Total Environ. 407 (9), 3153–3164. http://dx.doi.org/10.1016/j.scitotenv.2008.06.064.
Terzaghi, K., 1943. Theoretical Soil Mechanics. John Wiley & Sons, Inc., p. 265.
Wright, P., Stow, R., 1999. Detecting mining subsidence from space. Int. J. Remote Sens. 20 (6), 1183–1188.
Zebker, H.A., Goldstein, R.M., 1986. Topographic Mapping from interferometric synthetic aperture radar observations. J. Geophys. Res. 91, 4993–4999.
Zhong, L., Danskin, W.R., 2001. InSAR analysis of natural recharge to define structure of a ground-water basin, San Bernardino. Geophys. Res. Lett. 28 (13), 2661–2664.